Robbins, B. A. & Griffiths, D. V. (2019). *Géotechnique* **69**, No. 2, 174–179 [https://doi.org/10.1680/jgeot.17.P.209]

TECHNICAL NOTE

A new fragment for seepage beneath impervious structures

B. A. ROBBINS* and D. V. GRIFFITHS†

A new fragment type is developed using finite elements, with results presented in the form of charts for the estimation of seepage beneath levees and other water-retaining structures. The chart solutions are then compared with existing approximate solutions based on blanket theory. The charts are shown to agree well with existing methods, while including the option of anisotropic permeability, levee embedment, narrower levees and finite widths of the seepage zones. The charts are also shown to be useful in finite-element mesh design, by indicating the minimum distance needed in the mesh to model an infinite boundary.

KEYWORDS: embankments; finite-element modelling; groundwater; seepage

INTRODUCTION

The analysis of seepage beneath water-retaining structures has always been a subject of great practical importance for geotechnical engineers (Clibborn, 1902; Bligh, 1915; Casagrande, 1937; Harr, 1962; Bear, 1979). Accurate prediction of seepage quantities and uplift pressures is imperative to predicting the future performance of structures and, in the case of water storage projects, the life-cycle costs of operating the facility. Although finite-element analysis (FE) offers a powerful means of assessing seepage for general geometries and soil properties, recent attention (Meehan & Benjasupattananan, 2012, 2013; Batool *et al*., 2015) for relatively simple geometries has focused on semi-analytical solutions such as blanket theory for underseepage analysis, owing to its convenience, simplicity and accuracy.

Batool *et al*. (2015) provide an excellent review of a family of blanket theory solutions developed by the U.S. Army Corps of Engineers (USACE, 1956, 2000). As blanket theory is based on the 'method of fragments' (e.g. Harr, 1962; Holtz & Kovacs, 1981; Griffiths, 1984; Griffiths & Li, 1986), the analytical solutions perform well as long as the assumptions for the fragments are met (i.e. equipotentials are assumed to be vertical at key locations). This study presents a new fragment for the convenient solution of underseepage problems that closely agrees with blanket theory, but with the additional capability of being able to account for anisotropy, levee embedment, narrower levees and finite widths of the seepage zones.

REVIEW OF BLANKET THEORY

Blanket theory refers to a family of semi-analytical solutions presented collectively for the first time by Turnbull & Mansur (1959) in a paper focused on levee underseepage. Two particular cases considered in blanket theory together with their flow nets are illustrated in Fig. 1. The foundation is of finite depth, as are the distances to both the left and right boundaries. The upstream boundaries (left vertical boundary and ground surface) are constant head boundaries with the total head fixed at the upstream water surface elevation. The downstream boundaries (right vertical boundary and ground surface in Fig. 1(a), and right vertical boundary in Fig. 1(b)) are also constant head boundaries with the total head set to the ground surface elevation. As levees are typically constructed in fluvial depositional environments, it is quite common for levee foundations to consist of coarse-grained channel deposits overlain by fine-grained flood deposits forming a confining layer, or 'blanket', as shown. The common presence of this blanket layer within levee foundations is what led to the term blanket theory.

The cases shown in Fig. 1 can be generalised into seven distinct cases depending on the relative permeability and presence of the confining layer, as summarised in Table 1. This paper focuses on cases 1 to 4, but for further discussion of cases 5 to 7, the interested reader may refer to Meehan & Benjasupattananan (2012) and Batool *et al*. (2015). For cases 1 to 4, the levee cross-section is decomposed into two basic fragment types, as shown in Fig. 1, involving a type I fragment (Harr, 1962), which has a trivial form factor equal to the aspect ratio of the rectangular domain, where $\Phi = L_2/\mathrm{D}$ in case 1 or $\Phi = (L_2 + L_3)/\mathrm{D}$ in case 4, plus a special 'corner fragment' that assumes a vertical equipotential under the edge of the levee. This corner fragment is not a standard fragment type, but still has a well-known analytical solution given by $\Phi = 0{\cdot}43$, as will be discussed in the following section. It may be noted that the fragment types I, IV, V and VI proposed by Harr (1962) were later rationalised into a single 'type B' fragment by Griffiths (1984). The form factors for cases 1 to 4 are then easily determined according to blanket theory, as shown in Table 1. As case 2 is simply one-dimensional flow through the foundation, the corresponding form factor in Table 1 is entirely trivial and will not be discussed further. As noted by Batool *et al*. (2015), these form factors are sufficiently accurate provided the length of the top impervious boundary is greater than the depth of the aquifer (i.e. with reference to Figs 1(a) and 1(b), $L_2 \geq \mathrm{D}$ for case 1 and $L_2 + L_3 \geq \mathrm{D}$ for case 4, respectively). The reason for this limitation will become clear from the discussion of the analytical and finite-element solutions in the following section.

Manuscript received 17 August 2017; revised manuscript accepted 13 March 2018. Published online ahead of print 19 April 2018. Discussion on this paper closes on 1 July 2019, for further details see p. ii.

* U.S. Army Engineer Research and Development Center, Vicksburg, MS, USA (Orcid:0000-0002-4758-1450).
† Colorado School of Mines, Golden, CO, USA.

Downloaded by [SAN 301-9268 CO SCH MINES] on [23/01/19]. Copyright © ICE Publishing, all rights reserved.

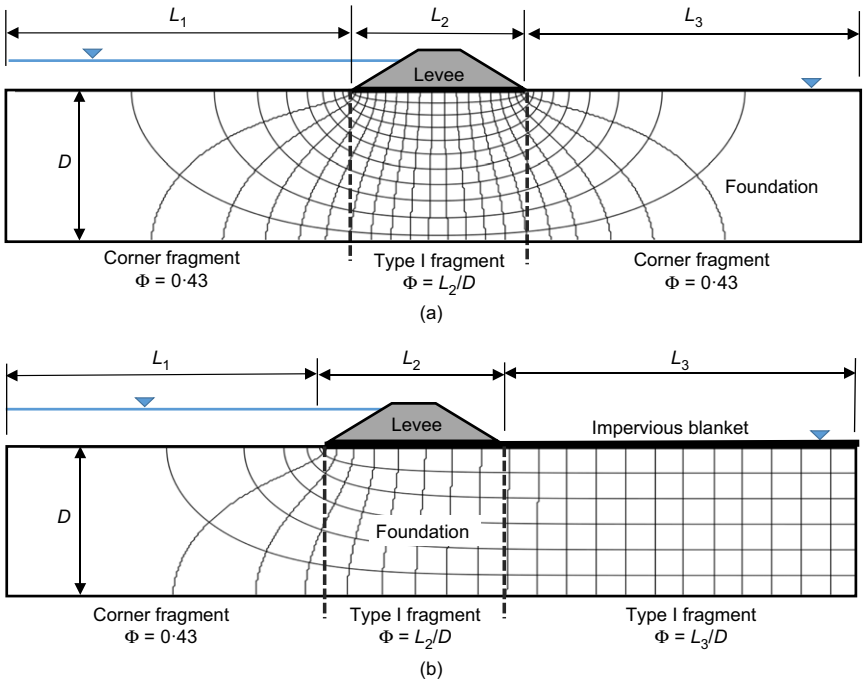

Fig. 1. Levee cross-section for underseepage analysis in blanket theory: (a) case 1; (b) case 4 (and case 3)

Table 1. Summary of blanket theory cases

Case	Riverside condition	Landside condition	Form factor (Φ)
1	No blanket	No blanket	$L_2/D + 0{\cdot}86$
2	Impervious blanket	Impervious blanket	$(L_1 + L_2 + L_3)/D$
3	Impervious blanket	No blanket	$(L_1 + L_2)/D + 0{\cdot}43$
4	No blanket	Impervious blanket	$(L_2 + L_3)/D + 0{\cdot}43$
5	Semipervious blanket	No blanket	(see Batool *et al.*, 2015)
6	No blanket	Semipervious blanket	(see Batool *et al.*, 2015)
7	Semipervious blanket	Semipervious blanket	(see Batool *et al.*, 2015)

ANALYTICAL SOLUTION – CASE 1

Muskat (1937) derived an exact analytical solution for case 1 (Fig. 1(a)), resulting in the following equation for the quantity of seepage beneath the embankment

$$Q = \frac{kHK'}{2K}, \quad m = \tanh\left(\frac{\pi L_2}{4D}\right) \tag{1}$$

where k is the (isotropic) permeability of the foundation and H is the head loss across the structure. K and K' are the complete elliptic integrals of the first kind with modulus m (and corresponding co-modulus). This exact analytical solution has been inconvenient to use in practice because the values for the elliptic integrals had to be looked up in tables. An approximate solution that does not require the use of the elliptic integrals was developed even earlier by Forchheimer (1917), as shown in equation (2).

$$Q = -\frac{kH}{2\pi}\log\left[\frac{\cosh(\pi L_2/8D) - 1}{3\cosh(\pi L_2/8D) - 1}\right] \quad \text{for} \quad \left(\frac{L_2}{D}\right) < 1$$
$$Q = \frac{kH}{(0{\cdot}86 + L_2/D)} \quad \text{for} \quad \left(\frac{L_2}{D}\right) \geq 1 \tag{2}$$

From equation (2), the total form factor for the system given by case 1 can easily be back-figured using its fundamental definition given by

$$\Phi = \frac{kH}{Q} \tag{3}$$

The approximate solutions developed by Forchheimer (1917) were central to the development of blanket theory, as they led to the form factor used for the 'corner fragments'. Through comparison of equation (2) to the form factor for case 1 from Table 1, it is seen that the case 1 form factor from blanket theory is identical to the Forchheimer form factor when $L_2/D \geq 1$. As the type I fragment has a trivial form factor given by $\Phi = L_2/D$, the form factor for each of the two 'corner fragments' can be calculated as

$$\Phi_{\text{corner}} = \frac{\Phi_{\text{total}} - (L_2/D)}{2} = \frac{0{\cdot}86}{2} = 0{\cdot}43 \tag{4}$$

Thus, it is readily seen that the blanket theory restriction that $L_2/D \geq 1$ stems from the Forchheimer equations. It should be noted that all of these solutions assume that the seepage zones extend to the far-field ($L_1 = L_3 = \infty$) in both the up- and down-stream directions. The potential error in the blanket theory solution due to the corner fragment assumption ($L_2/D \geq 1$) being violated can be evaluated directly by comparing the exact form factor from equation (1) to the form factors based on blanket theory for case 1 as given in Table 1. From equation (1), the exact total form factor for case 1 is easily determined to be

$$\Phi = 2K/K' \tag{5}$$

A comparison of Muskat's exact solution, Forchheimer's approximate solution and blanket theory case 1 is provided in Fig. 2 for a range of L_2/D values, including $L_2/D < 1$.

Downloaded by [SAN 301-9268 CO SCH MINES] on [23/01/19]. Copyright © ICE Publishing, all rights reserved.

The case 1 blanket theory solution begins to diverge from Muskat and Forchheimer at an L_2/D ratio between 0·8 and 1, increasing to an error of 10% at $L_2/D = 0{\cdot}2$ and 17% at $L_2/D = 0{\cdot}1$. This confirms that the accuracy of blanket theory is optimal when $L_2/D \geq 1$.

COMPARISONS WITH FINITE ELEMENTS

As the corner fragment derivation assumes the seepage zones extend to the far field in both the up- and downstream directions, it is also of interest to assess the influence of the finite L_1 and L_3 dimensions used in blanket theory on the error in predicted flow rates by way of detailed finite-element analyses of case 1 over a range of geometries. For example, how far would L_1 and L_3 have to extend (relative to D) to be essentially 'infinite'? As case 1 is symmetric, only half of the problem was modelled. The problem geometry and an example mesh are illustrated in Fig. 3. The analysis was performed using a modified version of the finite-element program for steady-state, planar flow described in Smith & Griffiths (2004). The mesh density indicated in the figure was shown to give very satisfactory accuracy. The base width of the embankment ($L_2 = 2b$) was fixed to a distance of 40 m ($b = 20$ m in Fig. 3). The foundation depth was then varied to achieve various L_2/D ratios. $L_1 (= L_3)$ was varied to achieve various L_2/L_T ratios where L_T is the total model width given by $L_T = L_1 + L_2 + L_3$. For each analysis, the flow rate was computed by summing the horizontal flux perpendicular to the centreline of the embankment. The form factor was then calculated as

$$\Phi_{FEM} = \frac{kH}{Q_{FEM}} \tag{6}$$

For each analysis, the blanket theory form factor was also computed by using the equation in Table 1. The relative error in the blanket theory form factor was then calculated for every combination of parameters as

$$\varepsilon(\%) = 100(\Phi_{BT} - \Phi_{FEM})/\Phi_{FEM} \tag{7}$$

The relative error in the form factor predicted by blanket theory over a range of possible geometries is shown in Fig. 4, indicating that the error is more sensitive to the distance to the model boundary (L_2/L_T) than to the ratio of L_2/D. For example, for $L_2/L_T = 0{\cdot}4$ and $L_2/D = 0{\cdot}35$, blanket theory over-predicts the form factor (and hence under-predicts the flow rate Q) by 50% as opposed to the <5% error in the case of infinite model lengths. A 5% error contour for equation (2) was also plotted (Fig. 4). Because of the corner fragment assumption (Fig. 2), the error in blanket theory remains higher than equation (2) error for low L_2/L_T ratios. Equation (2) exhibits a slight discontinuity at $L_2/D = 1$ due to the change in equations, after which blanket theory and equation (2) result in identical errors due to the corner fragment assumption being satisfied. The error in cases 3 and 4 by blanket theory is approximately half of the error illustrated in Fig. 4 for case 1.

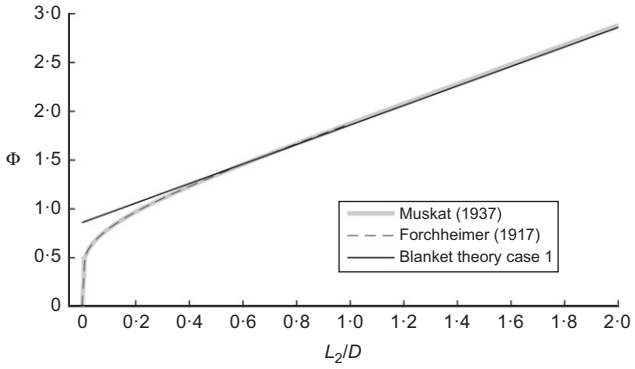

Fig. 2. Comparison of blanket theory case 1 to analytical solutions

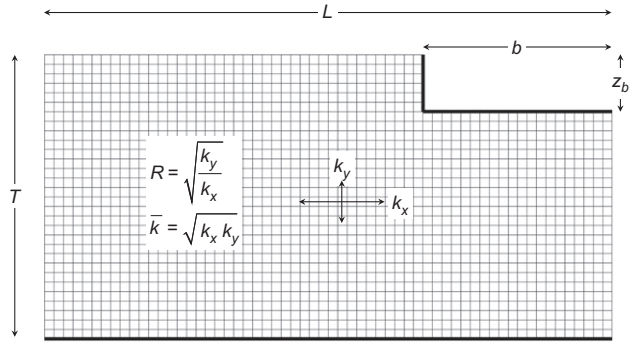

Fig. 3. Finite-element model and type D fragment geometry for underseepage. Dimensionless groups: *bR/T*, *b/L*, *z_b/T*

A NEW FRAGMENT FOR UNDERSEEPAGE ANALYSES

While the finite-element method offers the most powerful and general method of analysis for steady seepage

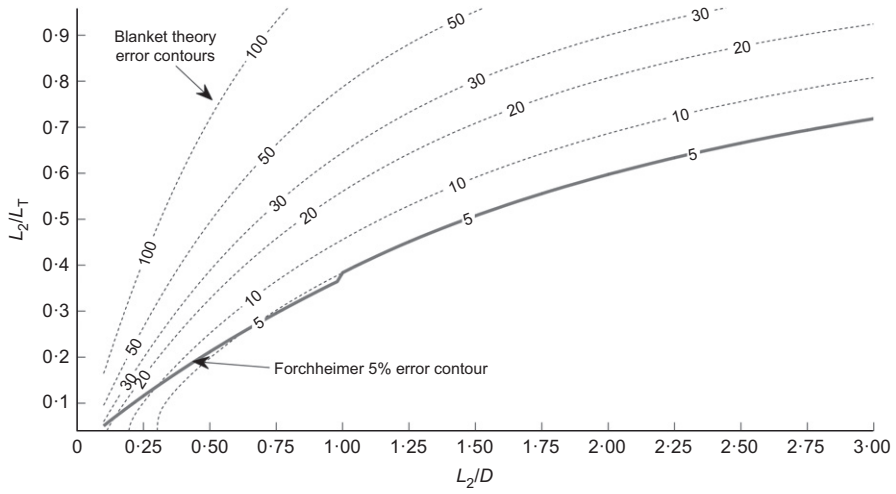

Fig. 4. Percentage error in blanket theory case 1 prediction for a broad range of geometries

Downloaded by [SAN 301-9268 CO SCH MINES] on [23/01/19]. Copyright © ICE Publishing, all rights reserved.

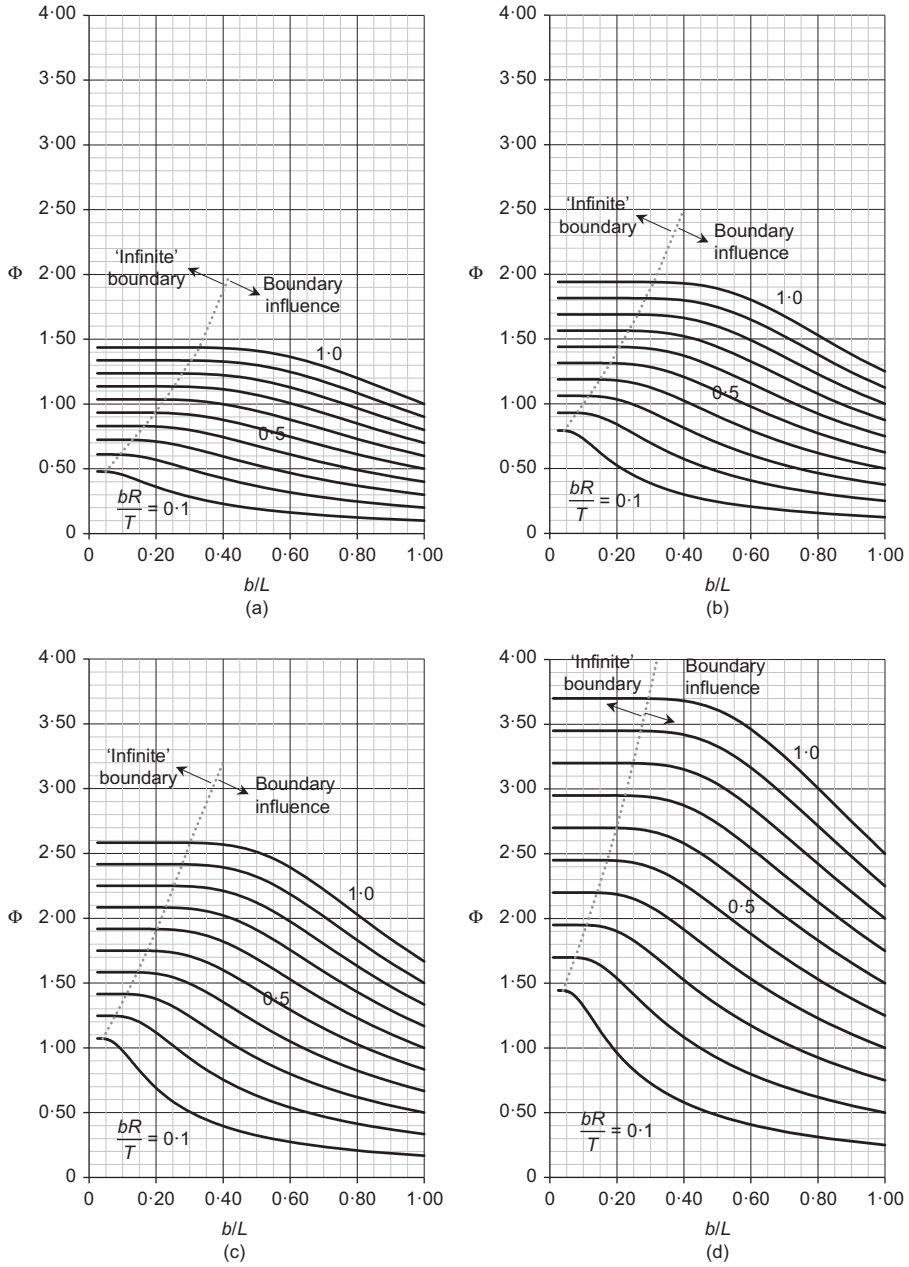

Fig. 5. Type D fragment chart for: (a) $z_b/T = 0{\cdot}0$; (b) $z_b/T = 0{\cdot}2$; (c) $z_b/T = 0{\cdot}4$; (d) $z_b/T = 0{\cdot}6$

problems, for the relatively simple geometries described in cases 1 to 4, a new fragment was developed as a quick and accurate alternative for assessing seepage beneath impervious structures. The geometry of the new fragment is illustrated in Fig. 3 and will be referred to as a 'type D' fragment with a total width L, total foundation depth T and levee half-width b (equivalent to $L_1 + L_2/2$, D and $L_2/2$, respectively, from Fig. 1) for consistency with fragment types A, B and C previously described by Griffiths (1984). In addition, the depth of embedment of the levee beneath ground level is given by z_b.

Approximately 16 000 finite-element analyses were conducted to cover a wide range of geometry configurations for this fragment, leading to Fig. 5. It may also be noted that the new fragment accounts for anisotropic permeability where $k_x \neq k_y$ by way of an anisotropy factor given by

$$R = \sqrt{\frac{k_y}{k_x}} \tag{8}$$

and an equivalent permeability given by

$$\bar{k} = \sqrt{k_x k_y} \tag{9}$$

Focusing for the time being on the case of no levee embedment (i.e. $z_b = 0$), Fig. 5(a) covers blanket widths in the range $0{\cdot}1 \leq (bR/T) \leq 1$. Noting the case of $b/L = 0{\cdot}0$ corresponds to the conditions of $(L_1 = L_3 = \infty)$, it is readily seen from Fig. 5 how the form factor (and hence flow rate) varies with increasing values of b/L due to the increasing boundary influence. For low b/L ratios, the boundary acts as a far-field, or 'infinite', boundary leading to constant form factors. The portions of the charts satisfying the 'infinite' boundary conditions were delineated by connecting the points on the fragment curves at which the form factor deviated 0·001 from the infinite condition of $b/L = 0{\cdot}0$. The delineating lines can be used as a guide for designing finite-element meshes with far-field boundaries, as will be demonstrated in the example application.

Cases 1, 3 and 4 of blanket theory can all be represented using the type D fragment. For case 1, the solution by symmetry is a superposition of two type D fragments where

Downloaded by [SAN 301-9268 CO SCH MINES] on [23/01/19]. Copyright © ICE Publishing, all rights reserved.

$b = L_2/2$. For cases 3 and 4, the problem can be represented by a single type D fragment in which the distance $b = L_1 + L_2$ or $b = L_2 + L_3$. By using a type D fragment to assess these cases, any boundary distance (L_1 or L_3) and any levee width ratio (L_2/D) may be assessed accurately.

Considering now the case of embedment (i.e. $z_b > 0$), Figs 5(b)–5(d) demonstrate that embedment has a significant effect on the flow rate. For example, taking the case of $bR/T = 0{\cdot}5$ with lateral seepage boundaries in the far field, the form factor with $z_b/T = 0$ from Fig. 5(a) is given as $\Phi \approx 0{\cdot}93$ and with $z_b/T = 0{\cdot}2$ from Fig. 5(b) as $\Phi \approx 1{\cdot}32$, some 42% higher (implying a flow rate some 42% lower). To review this influence in more detail, an additional set of finite-element runs was performed in the range $0 \leq z_b/T \leq 0{\cdot}6$ for the cases of $bR/T = 0{\cdot}5$ and $bR/T = 1$ with the lateral boundaries in the far field. The results, shown in Fig. 6, clearly indicate the benefits of embedment, especially if flow rate mitigation is a priority.

EXAMPLE APPLICATION OF THE FRAGMENT CHARTS

Figure 7 shows a concrete gravity structure resting on a homogeneous foundation extending to the far field in the upstream and downstream directions. Consider first the case of no embedment in which $z_b = 0$ and $k_x = k_y$, where, accounting for symmetry

$$\frac{z_b}{T} = 0{\cdot}0 \quad \text{and} \quad \frac{bR}{T} = 0{\cdot}5 \tag{10}$$

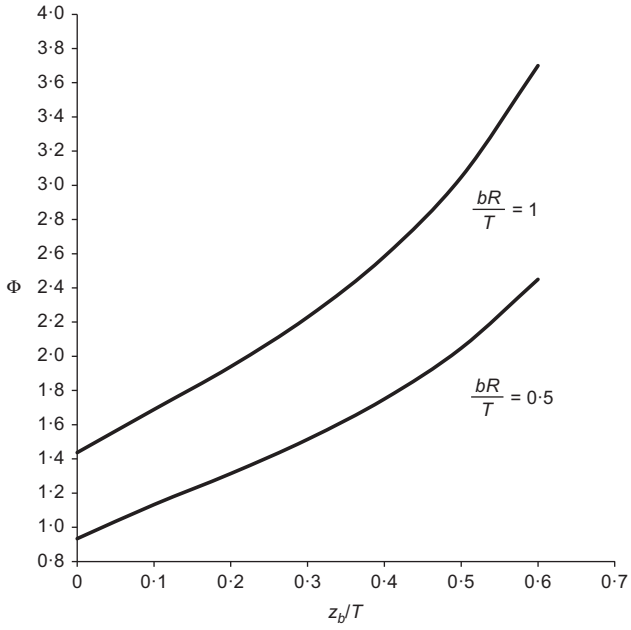

Fig. 6. Influence of levee embedment on case 1 form factors

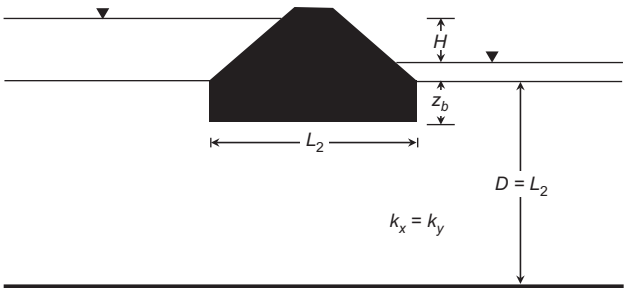

Fig. 7. Example application geometry

This example includes no blanket, and the permeable soil on both sides extends to the far field. From Fig. 5, the form factor is given by $\Phi \approx 0{\cdot}93$, indicating a flow rate by symmetry given by

$$Q = \frac{1}{2}\left(\frac{\bar{k}H}{0{\cdot}93}\right) = \frac{\bar{k}H}{1{\cdot}86} \tag{11}$$

where $\bar{k} = k_x = k_y$, which is essentially the same as the form factor given by case 1 of blanket theory of $\Phi \approx 1{\cdot}86$. Now consider the case in which $z_b = 0{\cdot}2L_2$ and $k_x = 4k_y$. Accounting again for symmetry with $R = 1/2$

$$\frac{z_b}{T} = 0{\cdot}2 \quad \text{and} \quad \frac{bR}{T} = 0{\cdot}25 \tag{12}$$

for which the form factor from Fig. 5 is given by $\Phi \approx 1{\cdot}0$, indicating a flow rate of

$$Q = \frac{1}{2}\left(\frac{\bar{k}H}{1{\cdot}0}\right) = \frac{\bar{k}H}{2{\cdot}0} \tag{13}$$

which is roughly 9% lower than in equation (11) due to the embedment and anisotropy. Blanket theory cannot compute the form factor for this case.

Lastly, consider the case in which it is desired to create a finite-element model of the scenario illustrated in Fig. 7 with $z_b = 0{\cdot}0$ and $R = 1{\cdot}0$. To determine what distance to use in the finite-element model to represent far-field boundaries, Fig. 5 can be used. For this particular problem, $bR/T = L_2/2D = 0{\cdot}5$, from which it is seen in Fig. 5 that an infinite boundary is obtained if $b/L = L_2/L_T < 0{\cdot}23$. This implies that the distance to the far-field boundaries must be at least $1{\cdot}67L_2$. To test this concept, a finite-element model was run for the situation in Fig. 7 with the distance to the boundary being $1{\cdot}67L_2$ and $10L_2$. The difference in the finite-element form factors for the two boundary distances was only 0·3%, confirming $1{\cdot}67L_2$ is indeed a suitable distance for simulating 'infinite' boundaries.

CONCLUSIONS

This paper has reviewed the analytical solution of Muskat, the semi-analytical solutions of Forchheimer and blanket theory for the calculation of seepage beneath levees and other water-retaining structures. The accuracy of blanket theory was confirmed in cases in which the lateral boundaries were in the far field and in which the levee width was at least as great as the depth of the permeable layer immediately below it. To enhance these traditional solutions, a new fragment (type D) was developed by finite-element analysis and presented in the form of charts giving the form factor for different geometries. The charts were shown to agree closely with blanket theory, but offered greater generality by including the option of anisotropic soil properties, levee embedment, relatively narrow levees and lateral confinement. The charts were also demonstrated to be useful in designing finite-element meshes to include far-field, or 'infinite', boundaries.

ACKNOWLEDGEMENT

Permission to publish was granted by the Director, Geotechnical and Structures Laboratory, U.S. Army Engineer Research and Development Center, Vicksburg, MS, USA.

NOTATION

b horizontal seepage length in new fragment (m)
D depth of soil domain in blanket theory (m)

Downloaded by [SAN 301-9268 CO SCH MINES] on [23/01/19]. Copyright © ICE Publishing, all rights reserved.

H differential head across a structure (m)
K complete elliptic integral of the first kind with modulus m
K' complete, complementary elliptic integral of the first kind with modulus m
k soil hydraulic conductivity (m/s)
k_x soil hydraulic conductivity in the x direction (m/s)
k_y soil hydraulic conductivity in the y direction (m/s)
$\bar{k}$ equivalent permeability for anisotropic soil (m/s)
L horizontal length of the seepage domain in new fragment (m)
L_T total seepage length in blanket theory (m)
L_1 upstream seepage length in blanket theory (m)
L_2 width of the embankment in blanket theory (m)
L_3 downstream seepage length in blanket theory (m)
m modulus for evaluating elliptic integrals of the first kind
Q total flow rate through a cross-section ($m^3/(s/m)$)
R anisotropic permeability factor
T depth of the soil domain in new fragment (denoted D in blanket theory) (m)
z_b embedment depth in the new fragment (m)
ε error in the blanket theory predictions (%)
Φ cross-sectional form factor for seepage quantity

REFERENCES

Batool, A., VandenBerge, D. R. & Brandon, T. L. (2015). Practical application of blanket theory and the finite-element method to levee underseepage analysis. *J. Geotech. Geoenviron. Engng* **141**, No. 4, 1–10, https://doi.org/10.1061/(ASCE)GT.1943-5606.0001269.

Bear, J. (1979). *Hydraulics of groundwater*, 1st edn. New York, NY, USA: Mcgraw-Hill, Inc.

Bligh, W. G. (1915). *Dams and weirs*. Chicago, IL, USA: American Technical Society.

Casagrande, A. (1937). Seepage through dams. *J. New England Water Works Ass.* **51**, No. 2, 295–337.

Clibborn, J. (1902). *Experiments on the passage of water through sand*. Technical Paper 97. Roorkee, India: Thomason College.

Forchheimer, P. (1917). Zur Grundwasserbewegung nach isothermischen Kurvenscharen. *Sitzber. kais. Akad. d. Wiss. Wien, Abt. IIa* **126**, No. 4, 409–440 (in German).

Griffiths, D. V. (1984). Discussion: rationalized charts for the method of fragments applied to confined seepage. *Géotechnique* **34**, No. 2, 229–238, https://doi.org/10.1680/geot.1985.35.3.375.

Griffiths, D. V. & Li, C. O. (1986). Finite element assessment of the method of fragments for problems of confined seepage. In *Proceedings of the 6th international conference on finite elements in water resources* (ed. A. S. Costa), pp. 143–152. Berlin, Germany: Springer.

Harr, M. E. (1962). *Groundwater and seepage*. New York, NY, USA: McGraw-Hill Book Company.

Holtz, R. D. & Kovacs, W. D. (1981). *An introduction to geotechnical engineering*. Englewood Cliffs, NJ, USA: Prentice-Hall.

Meehan, C. L. & Benjasupattananan, S. (2012). An analytical approach for levee underseepage analysis. *J. Hydrol.* **470–471**, No. 4, 201–211, https://doi.org/10.1016/j.jhydrol.2012.08.050.

Meehan, C. L. & Benjasupattananan, S. (2013). Analytical approach for modeling axisymmetric levee underseepage. *J. Geotech. Geoenviron. Engng* **140**, No. 4, 1–12, https://doi.org/10.1061/(ASCE)GT.1943-5606.0000952.

Muskat, M. (1937). *The flow of homogeneous fluids through porous media*, 1st edn. New York, NY, USA and London, UK: McGraw-Hill Book Company.

Smith, I. M. & Griffiths, D. V. (2004). *Programming the finite element method*, 4th edn. Hoboken, NJ, USA: John Wiley & Sons, Inc.

Turnbull, W. J. & Mansur, C. I. (1959). Investigation of underseepage – Mississippi River levees. *ASCE J. Soil Mech. Found. Div.* **85**, No. 4, 41–94.

USACE (United States Army Corps of Engineers) (1956). *Investigation of underseepage and its control, lower Mississippi River levees (TM-3-424)*. Vicksburg, MS, USA: U.S. Army Waterways Experiment Station.

USACE (2000). *Design and construction of levees (EM 1110-2-1913)*. Washington, DC, USA: USACE.

Downloaded by [SAN 301-9268 CO SCH MINES] on [23/01/19]. Copyright © ICE Publishing, all rights reserved.